JOURNAL OF AGRICULTURAL AND FOOD CHEMISTRY



Agricultural and Environmental Chemistry

# Design, Synthesis, Antiviral Bioactivity and Defense Mechanisms of Novel Dithioacetal Derivatives Bearing a Strobilurin Moiety

Jin Chen, Jing Shi, Lu Yu, Dengyue Liu, Xiuhai Gan, Song Baoan, and De-Yu Hu

*J. Agric. Food Chem.*, **Just Accepted Manuscript** • DOI: 10.1021/acs.jafc.8b01297 • Publication Date (Web): 09 May 2018



ACS Publications

is published by the American Chemical Society. 1155 Sixteenth Street N.W., Washington, DC 20036

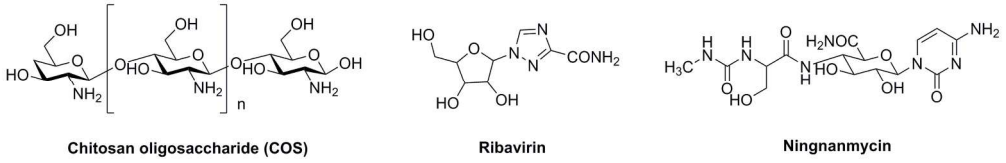


Figure 1 Chemical structures of Chitosan oligosaccharide, Ribavirin, and Ningnanmycin.

189x30mm (300 x 300 DPI)

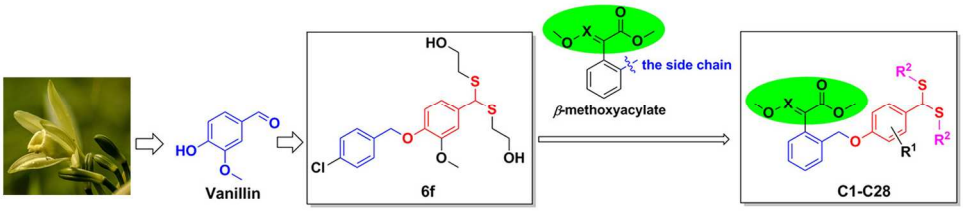


Figure 2. Design of the title compounds.

177x38mm (300 x 300 DPI)

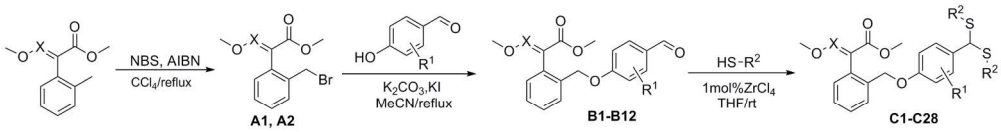


**C1**: $R^1$=2-$OCH_3$, $R^2$=2-hydroxyethyl, X=N
**C2**: $R^1$=2-$OCH_3$, $R^2$=Et, X=N
**C3**: $R^1$=2-$OCH_3$, $R^2$=4-F-Ph, X=N
**C4**: $R^1$=2-$OCH_3$, $R^2$=Bn, X=N
**C5**: $R^1$=H, $R^2$=2-hydroxyethyl, X=N
**C6**: $R^1$=H, $R^2$=Et, X=N
**C7**: $R^1$=2-$CH_3$, $R^2$=2-hydroxyethyl, X=N
**C8**: $R^1$=2-$CH_3$, $R^2$=Et, X=N
**C9**: $R^1$=2-OEt, $R^2$=Et, X=N
**C10**: $R^1$=2,6-di$OCH_3$, $R^2$=2-hydroxyethyl, X=N
**C11**: $R^1$=2,6-di$OCH_3$, $R^2$=Et, X=N
**C12**: $R^1$=2-Cl, $R^2$=2-hydroxyethyl, X=N
**C13**: $R^1$=2-Cl, $R^2$=Pr, X=N
**C14**: $R^1$=2-Cl, $R^2$=Et, X=N
**C15**: $R^1$=2-Cl, $R^2$=*i*-Pr, X=N
**C16**: $R^1$=2-Br, $R^2$=2-hydroxyethyl, X=N
**C17**: $R^1$=2-Br, $R^2$=Et, X=N
**C18**: $R^1$=2-Br, $R^2$=Pr, X=N
**C19**: $R^1$=2-Br, $R^2$=*i*-Pr, X=N
**C20**: $R^1$=3-Cl, $R^2$=2-hydroxyethyl, X=N
**C21**: $R^1$=3-Cl, $R^2$=Et, X=N
**C22**: $R^1$=3-$CH_3$, $R^2$=2-hydroxyethyl, X=N
**C23**: $R^1$=3-$CH_3$, $R^2$=Et, X=N
**C24**: $R^1$=3-$OCH_3$, $R^2$=2-hydroxyethyl, X=N
**C25**: $R^1$=3-$OCH_3$, $R^2$=Et, X=N
**C26**: $R^1$=2-Cl, $R^2$=Et, X=CH
**C27**: $R^1$=2-Cl, $R^2$=*i*-Pr, X=CH
**C28**: $R^1$=2-Br, $R^2$=Et, X=CH

Figure 3 Synthetic route of dithioacetal derivatives bearing strobilurin moiety.

174x73mm (300 x 300 DPI)

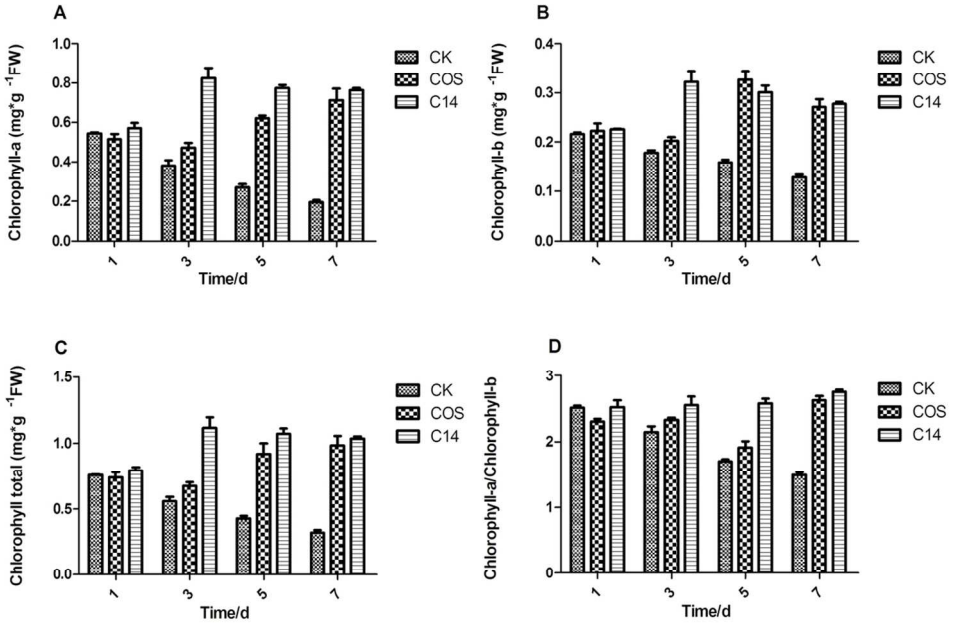


Figure 4 Effects of compound C14 on Ca (A), Cb (B), Ct (C), and Chlorophyll a/b (D) in tobacco leaves. Vertical bars refer to mean ± SD (n = 3).

54x38mm (600 x 600 DPI)

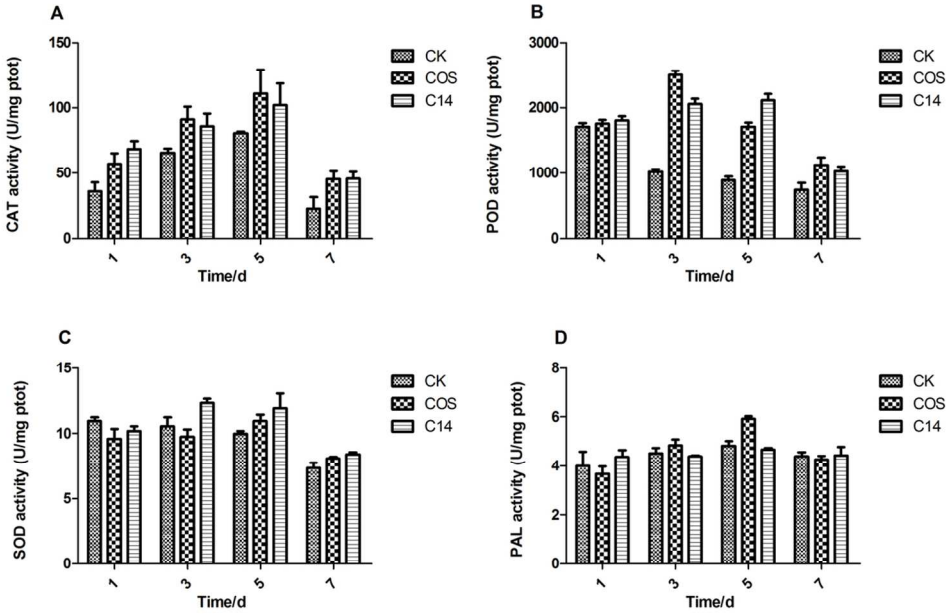


Figure 5. Effects of compound C14 on CAT (A), POD (B), SOD (C), and PAL (D) activity in tobacco leaves. Vertical bars refer to mean ± SD (n = 3).

54x36mm (600 x 600 DPI)

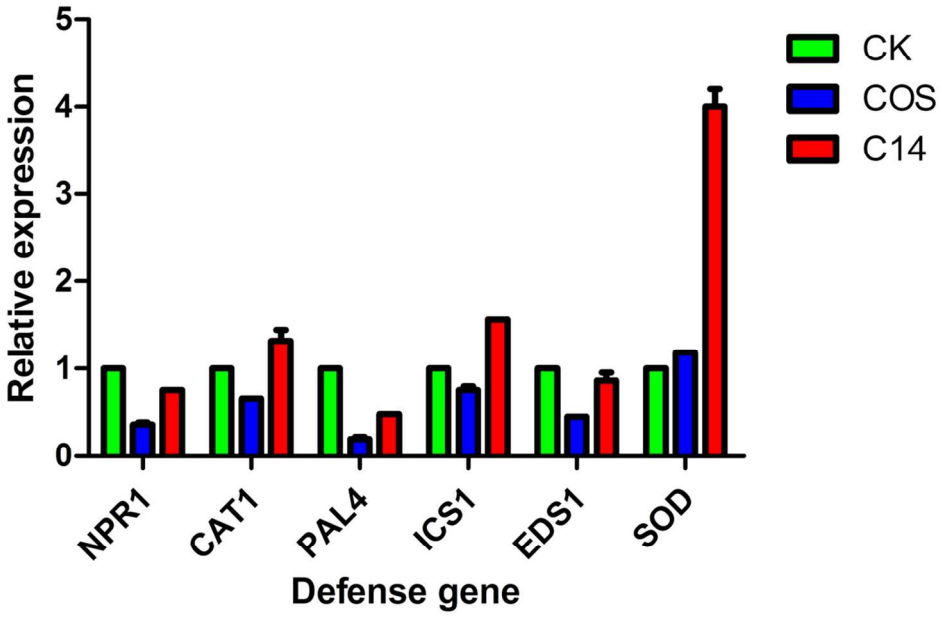


Figure 6. Gene expression analysis of the related genes by RT-qPCR. The genes expression levels of CAT-1, ICS-1, and SOD were up-regulated by C14 treatment.

54x36mm (600 x 600 DPI)

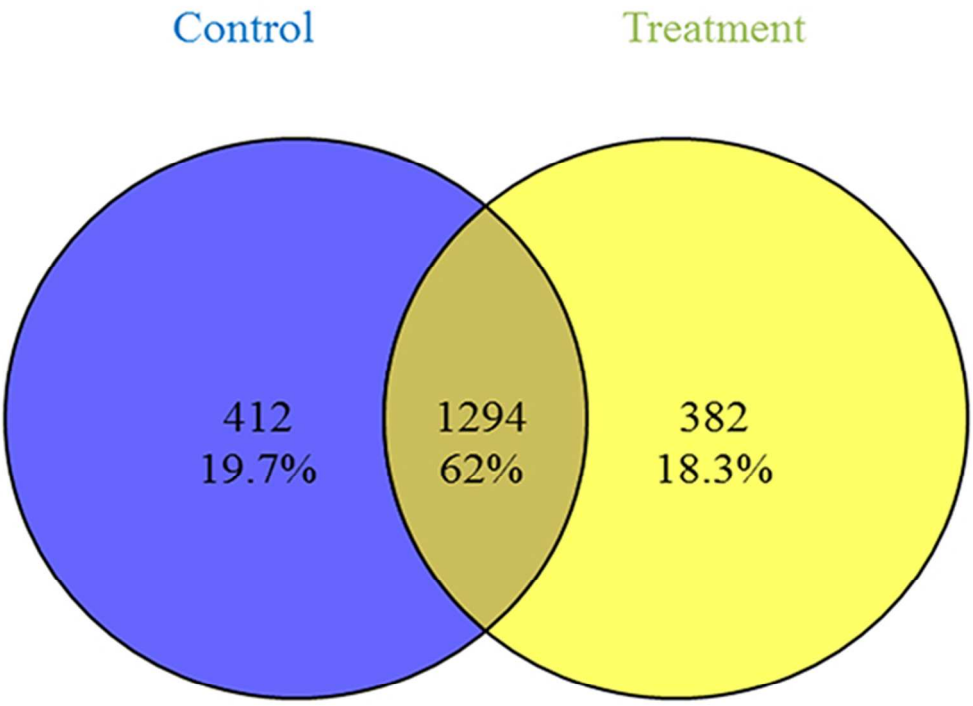


53x44mm (300 x 300 DPI)

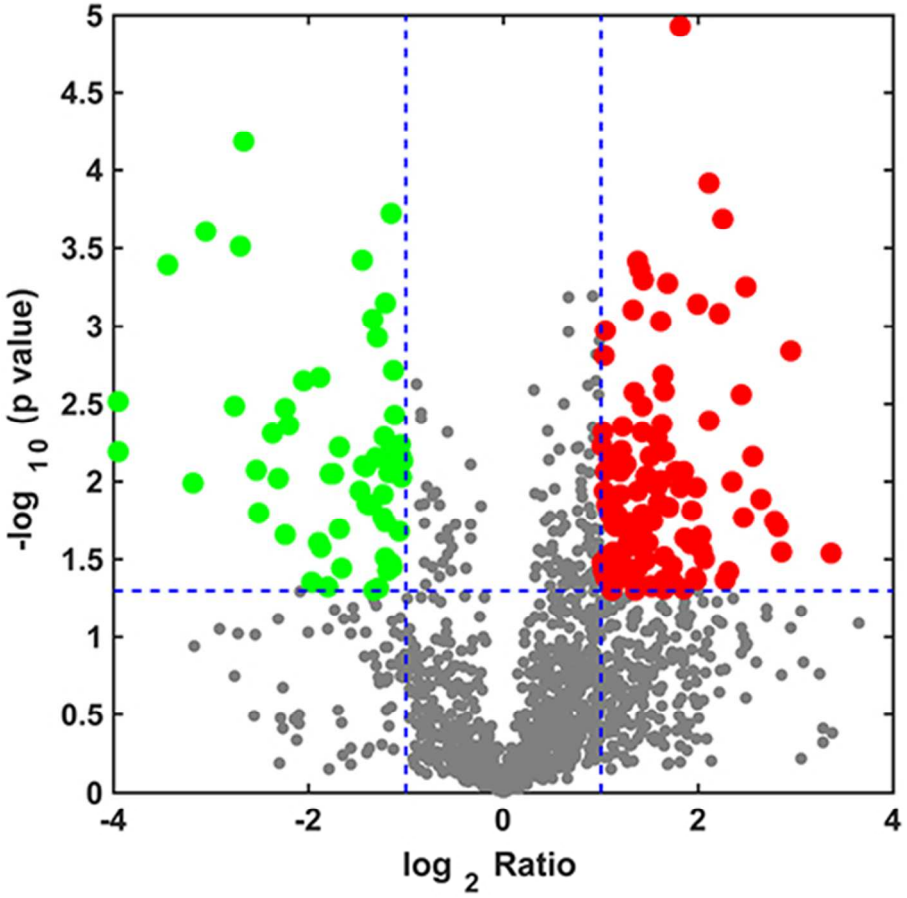


Figure 8. Volcano plot of the relative protein abundance changes between control group and treatment group. The red points are significant up-regulated proteins, while the green points are significant down-regulated protein.

45x44mm (300 x 300 DPI)

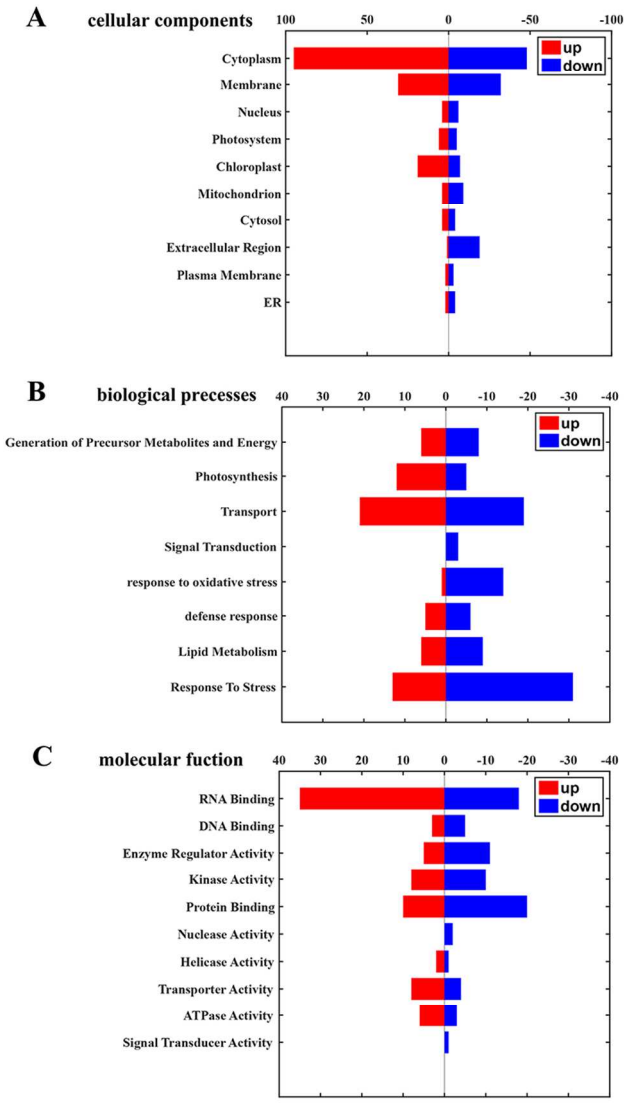


Figure 9. The differential expression proteins between control and treatment group were classified based on known cellular components (A), biological process (B) and molecular functions (C).

84x132mm (300 x 300 DPI)

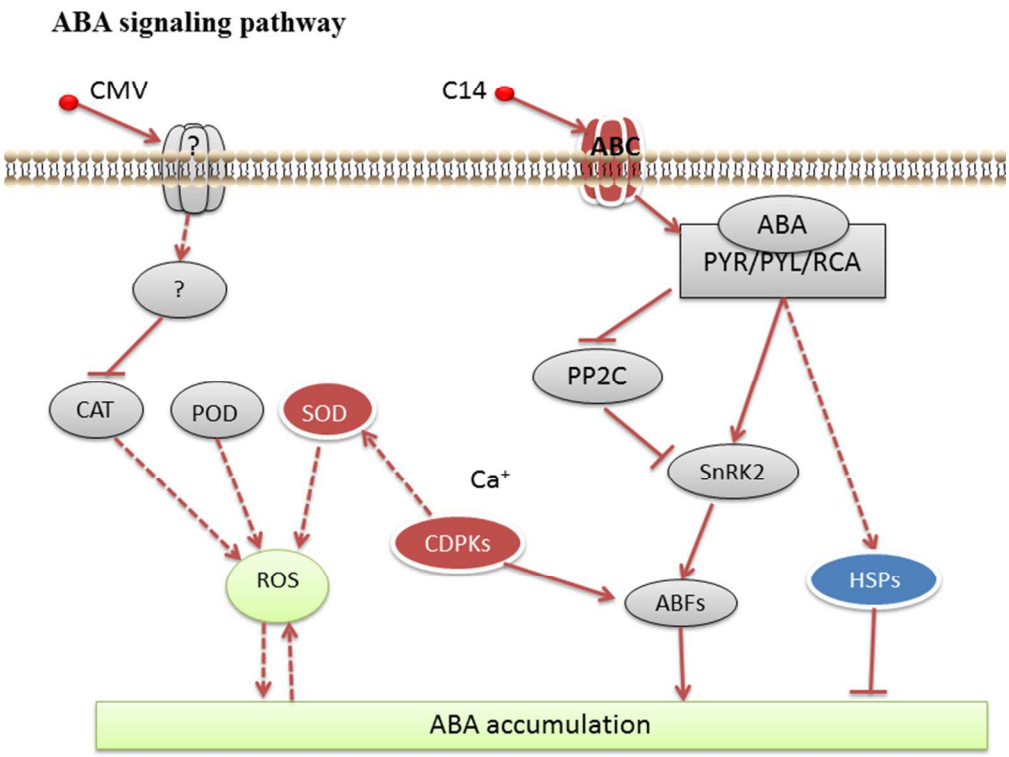


Figure 10. The ABA signaling pathway in tobacco response to C14. Red color represent up-accumulated proteins in this pathway, while the green color represent down-accumulated

144x112mm (300 x 300 DPI)

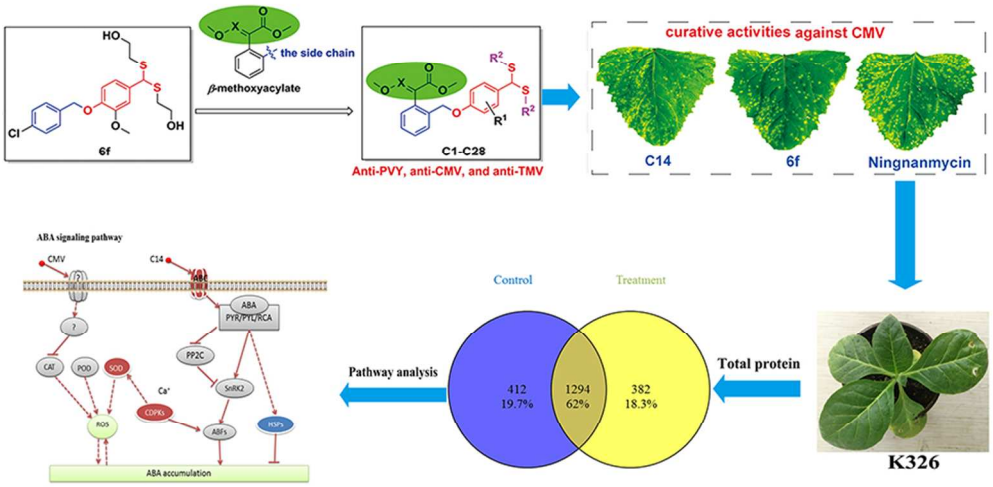


TOC Graphic

82x44mm (300 x 300 DPI)

# Design, Synthesis, Antiviral Bioactivity and Defense Mechanisms of Novel Dithioacetal Derivatives Bearing a Strobilurin Moiety

Jin Chen,[†] Jing Shi,[†] Lu Yu,[†] Dengyue Liu,[†] Xiuhai Gan,[†] Baoan Song,*[,†] Deyu Hu*[,†]

[†]State Key Laboratory Breeding Base of Green Pesticide and Agricultural Bioengineering, Key Laboratory of Green Pesticide and Agricultural Bioengineering, Ministry of Education, Guizhou University, Huaxi District, Guiyang 550025, China

*Corresponding author (Tel.: 86-851-88292170; Fax: 86-851-88292170; E-mail: dyhu@gzu.edu.cn; songbaoan22@yahoo.com)

**ABSTRACT**: A series of dithioacetal derivatives bearing a strobilurin moiety were designed and synthesized on the basis of our previous work. The antiviral activities of these compounds against Potato virus Y (PVY), Cucumber mosaic virus (CMV), and Tobacco mosaic virus (TMV) were systematically evaluated. Bioassay results indicated that **C14** elicited excellent curative and protective activities against PVY, CMV, and TMV. The former had 50% effective concentrations ($EC_{50}$) of 125.3, 108.9, and 181.7 μg/mL, respectively, and the latter had 148.4, 113.2, and 214.6 μg/mL, respectively, which were significantly superior to those of lead compound **6f** (297.6, 259.6, and 582.4 μg/mL and 281.5, 244.3, and 546.3 μg/mL, respectively), Ningnanmycin (440.5, 549.1, and 373.8 μg/mL and 425.3, 513.3, and 242.7 μg/mL, respectively), Chitosan oligosaccharide (553.4, 582.8, and 513.8 μg/mL and 547.3, 570.6, and 507.9 μg/mL, respectively), and ribavirin (677.4, 690.3, and 686.5 μg/mL and 652.7, 665.4, and 653.4 μg/mL, respectively). Moreover, defensive enzyme activities and RT-qPCR analysis demonstrated that the antiviral activity was associated with the changes of SOD, CAT, and POD activity in tobacco, which was proved by the related proteins of abscisic acid signaling pathway. This work provided a basis for further design, structural modification, and development of dithioacetal derivatives as new antiviral agents.

**KEYWORDS**: dithioacetal derivatives, strobilurin moiety, antiviral activity, potato virus Y, cucumber mosaic virus, tobacco mosaic virus, plant resistance

## INTRODUCTION

Vegetables, which constitute an important food component for humans, are susceptible to infection of various plant viruses, such as Potato virus Y (PVY), Cucumber mosaic virus (CMV), and Tobacco mosaic virus (TMV), and Tomato chlorosis virus (ToCV). These plant viruses are pathogenic and can infect almost all vegetables, including pepper, tomato, eggplant, and cucumber. Vegetable viral diseases can cause massive economic losses because they are difficult to control.[1–3] The annual losses of tomato infected with CMV in China account for 25%–50%.[4] Chemical methods are the main solutions to control vegetable viral diseases. Ningnanmycin and Ribavirin (Figure 1) are typically used to control vegetable viral disease but have unsatisfactory control effect.[5] Chitosan oligosaccharide (COS; Figure 1) is an biological regulator with environmentally friendly that can induce plant immunity, but its control effect on vegetable viral diseases is not ideal.[6] Considerable efforts have been devoted to developing new and effective plant virucides, but their agricultural use is restricted because of an unsatisfactory antiviral activity.[7–9] Therefore, new antiviral agents with increased efficiency are needed to be developed.

Dithioacetal and its derivatives have been extensively pharmacologically investigated because of their extensive biological activities, such as antibacterial, antileishmanial, antiviral, and antifungal.[10] In our previous work, the novel dithioacetal derivative **6f** (Figure 2) exert markedly increased curative and protective activities against and PVY CMV. However, the compound exhibits moderate or even decreased activity against TMV. Structure–activity relationships (SARs) analysis have revealed that the benzyl etherification of 4-OH was beneficial to increase the antiviral activities and halogen atom

53 substituted benzyl ether compounds exhibited better antiviral activities than others,
54 especially, chlorine atom-substituted benzyl ether. About different substitutions of
55 disulfide on dithioacetal, aryl group compound is more suitable for antiviral activities
56 than the alkyl group.[10] Therefore, the introduction of a unique pharmacophore through
57 benzyl etherification can be used to develop antiviral agents based on lead compound **6f**
58 with increased effectiveness and spectrum width.

59 Strobilurins are important fungicidal compounds containing *β*-methoxyacrylate
60 pharmacophore (Figure 2).[11] Certain strobilurin fungicides have been commercialized
61 because of their excellent characteristics, such as unique action mechanism, wide
62 fungicidal spectrum, low toxicity toward mammalian cells, and environmental
63 nonreactiveness.[12] Strobilurins exhibit other biological properties, including improved
64 crop physiology,[13] insecticidal,[14] acaricidal,[15] and herbicidal effects,[16] and induced
65 resistance.[17] Strobilurin as an essential pharmacophore, the modification of strobilurin
66 side chains is an effective approach to obtain new highly active analogs.[18, 19]

67 We proposed to introduce the increased-spectrum bioactive strobilurin group to
68 dithioacetal to obtain a series of novel dithioacetal derivatives bearing a strobilurin
69 moiety (Figure 2) and to further investigate the antiviral activities of dithioacetal
70 derivatives. The antiviral activities of these derivatives against PVY, CMV, and TMV
71 were systematically evaluated. Bioassay results showed that several title compounds
72 showed more full-scale and better antiviral activity than commercially available
73 Ningnanmycin, COS, and ribavirin. Compared with lead compounds **6f**, compound **C14**
74 not only has better antiviral activity against PVY and CMV, but also can be used to
75 control TMV. Moreover, the plant defense response mechanisms of **C14**, including

76 chlorophyll content, enzyme activities, and differential protein expression were
77 researched. For all as our knowledge, this work first demonstrated that **C14** could
78 enhance resistance of tobacco to virus. Thus, **C14** could be considered as a novel plant
79 virucide.

80 **MATERIALS AND METHODS**

81 **General Information.** All of the reagents were purchased from commercial suppliers
82 and used without further purification. All of the solvents were used without further
83 purification and drying before use. Thin-layer chromatography with UV detection was
84 conducted on silica gel $GF_{254}$. The melting points of the products were determined with a
85 WRX-4 microscopic melting point meter (Shanghai Yice Apparatus & Equipment Co.,
86 Ltd., China) with an uncorrected thermometer. $^{1}H$, $^{13}C$, and $^{19}F$ nuclear magnetic
87 resonance (NMR) spectra were recorded on a Bruker Ascend-400 spectrometer (Bruker,
88 Germany) and JEOL ECX-500 spectrometer (JEOL, Tokyo, Japan) in $CDCl_3$ or DMSO-
89 $d_6$ solution with tetramethylsilane as internal standard. High-resolution mass spectral
90 (HRMS) data were determined with Thermo Scientific Q Exactive (Thermo, USA).

91 **General Procedure for Preparation of Intermediates A1–A2 and B1–B12**

92 Intermediates **A1**–**A2** were prepared on the basis of a previously described method.[20] A
93 solution of intermediates **A1**–**A2** (8.74 mmol) and substituted 4-hydroxybenzaldehyde
94 (8.74 mmol) in acetonitrile (35 mL) was heated to reflux for 8–12 h in $K_2CO_3$ (100
95 mol.%) and KI (5 mol.%). After the reaction was completed, the solvent was removed by
96 vacuum. Then residue was extracted using ethyl acetate to obtain intermediates **B1**–**B12**.
97 The representative data for **B1** are shown below.

98 *(E)-methyl-2-(2-((4-formyl-2-methoxyphenoxy)methyl)phenyl)-2-(methoxyimino)acetate*

99 ***(B1)***. Yield: 3.00 g (96%); yellow solid; m.p. 78 °C–80 °C; $^{1}$H NMR (400 MHz, $CDCl_3$)
100 $\delta$ 9.83 (s, 1H, -CH=O), 7.54 (d, $J$ = 7.2 Hz, 1H, Ar-H), 7.45–7.38 (m, 3H, Ar-H), 7.35 (dd,
101 $J$ = 8.4, 2.0 Hz, 1H, Ar-H), 7.20 (dd, $J$ = 7.2, 0.8 Hz, 1H, Ar-H), 6.89 (d, $J$ = 8.4 Hz, 1H,
102 Ar-H), 5.11 (s, 2H, -$OCH_2$-), 4.04 (s, 3H, =N-$OCH_3$), 3.94 (s, 3H, -CO-$OCH_3$), 3.86 (s,
103 3H, Ar-$OCH_3$); $^{13}$C NMR (101 MHz, $CDCl_3$) $\delta$ 190.94 (1C), 163.23 (1C), 153.29 (1C),
104 150.03 (1C), 149.16 (1C), 134.42 (1C), 130.40 (1C), 129.78 (1C), 129.09 (1C), 128.49
105 (1C), 127.99 (1C), 127.35 (1C), 126.59 (1C), 112.35 (1C), 109.27 (1C), 69.00 (1C), 63.90
106 (1C), 56.04 (1C), 53.07 (1C); HRMS (ESI) *m/z* for $C_{19}H_{19}O_6NNa$ $[M+Na]^+$ calcd.
107 380.11046, found. 380.10980.

108 **General Procedure for the Synthesis of Dithioacetal Derivatives Bearing**
109 **Strobilurin (C1–C28).** $ZrCl_4$ (0.01 mmol) was added to a round-bottomed flask
110 containing intermediates **B1**–**B12** (1.40 mmol) and substituted mercaptane (2.80 mmol)
111 in THF solvent (3 mL). And then mixture was stirred at room temperature for 10–60
112 minutes. Vacuum removal of solvent after the reaction was completed. The mixture was
113 added to water and extracted with ethyl acetate thrice. The collected organic extracts were
114 dried, concentrated, and purified through silica gel column chromatography with a 3:1
115 (v/v) mixture of petroleum ether and ethyl acetate to obtain products **C1**–**C28**. The
116 representative data for **C1** are shown below.

117 *(E)-methyl-2-(2-((4-(bis(2-hydroxyethyl)dithioacetal)-2-methoxyphenoxy)methyl)phenyl)*
118 *-2-(hoxyimino)acetate (**C1**)*. Yield: 502 mg (72%); white solid; m.p. 61 °C–63 °C; $^{1}$H
119 NMR (400 MHz, $CDCl_3$) $\delta$ 7.54 (t, $J$ = 7.6 Hz, 1H, Ar-H), 7.44−7.35 (m, 2H, Ar-H), 7.18
120 (dd, $J$ = 7.2, 1.2 Hz, 1H, Ar-H), 7.03 (d, $J$ = 2.0 Hz, 1H, Ar-H), 6.85 (dd, $J$ = 8.4, 2.0 Hz,
121 1H, Ar-H), 6.70 (d, $J$ = 8.4 Hz, 1H, Ar-H), 5.02 (s, 1H, -SCHS-), 4.99 (s, 2H, Ar-$CH_2$O-),

122 4.04 (s, 3H, =N-$OCH_3$), 3.89 (s, 3H, -CO-$OCH_3$), 3.85 (s, 3H, Ar-$OCH_3$), 3.72 (t, $J$ = 5.9
123 Hz, 4H, -$CH_2$-), 2.85–2.77 (m, 2H, -$SCH_2$-), 2.74–2.67 (m, 2H, -$SCH_2$-), 2.51 (s, 2H, -
124 OH); $^{13}$C NMR (101 MHz, $CDCl_3$) $\delta$ 163.29 (1C), 149.90 (1C), 149.29 (1C), 147.87(1C),
125 135.26 (1C), 132.90 (1C), 129.67 (1C), 129.02 (1C), 128.30 (1C), 127.70 (1C), 127.50
126 (1C), 119.96 (1C), 113.24 (1C), 110.89 (1C), 69.02 (1C), 63.88 (1C), 61.36 (2C), 56.05
127 (1C), 52.97 (1C), 35.67 (2C); HRMS (ESI) *m/z* for $C_{23}H_{29}O_7NNaS_2$ $[M+Na]^+$ calcd.
128 518.12776, found. 518.12756.

129 **Antiviral Activity Assay.** *Purification of virus.* The *Nicotiana. tabacum* cv. K326
130 leaves inoculated with PVY, CMV and TMV were selected, and PVY,[21] CMV[22] and
131 TMV[23] were purified with the reported methods.

132 *Curative activities of the title compounds.* The leaves of and *Chenopodium*
133 *amaranticolor* and *N. tabacum* L. growing at the same ages were selected to evaluate the
134 anti-PVY[21], anti-CMV and anti-TMV activities[24]. The virus was dipped and inoculated on
135 the whole leaves, which were scattered with silicon carbide beforehand. After 1 h, the
136 leaves were washed with water and then dried. The compound solution was smeared on
137 the left side, and the solvent was smeared on the right side. The local lesion numbers were
138 recorded and antiviral activities were counted. Three repetitions were conducted for each
139 compound.

140 *Protective activities of the title compounds*. The compound solution was smeared on
141 the left side of the growing *C. amaranticolor* and *N. tabacum* L. leaves. The solvent was
142 smeared on the right side. The leaves were inoculated with virus after 1 day. Then, the
143 leaves were washed with water after inoculation for 2 h. The number of local lesions was
144 counted and inhibition rate of the compound was calculated.[21, 24] Three repetitions were

145 conducted for each compound.

146 **Physiology and Biochemistry of Tobacco.** *Compound Treatments and Sampling.*
147 *Nicotiana tabacum* cv. K326 of equally grown at the fourth leaf stage was selected. The
148 three treatments were CK, COS, and **C14**. CK was solvent and COS was used as negative
149 and positive controls, respectively. 500 μg/mL of **C14** solution were smeared on whole
150 leaves. After 12 h of spraying, the leaves of all of the plants were evenly inoculated with
151 CMV and cultured in a greenhouse. After the plants were inoculated with the virus, tissue
152 samples were collected 1, 3, 5, and 7 days after the treatment, then test and calculate the
153 content of chlorophyll and the activity of defense enzyme. All tests were repeated three
154 times.

155 *Chlorophyll Content Test.* Chlorophyll content was determined with chlorophyll assay
156 reagent kits in accordance with the manufacturer's instructions (Suzhou Comin
157 Bioengineering Institute, China). Absorbance spectra were obtained at 663 and 645 nm
158 for chlorophyll a ($C_a$) and chlorophyll b ($C_b$), respectively. $C_a$, $C_b$, total chlorophyll
159 content ($C_t$), and chlorophyll a/b were then calculated.

160 *Determination of Defensive Enzyme Activities.* Using enzyme assay reagent kits from
161 the manufacturer's instructions (Suzhou Comin Bioengineering Institute, China)
162 calculated the activities of catalase (CAT), peroxidase (POD), superoxide dismutase
163 (SOD), and phenylalanine ammonia lyase (PAL).

164 **Gene Expression Analysis.** The total RNA was extracted of the tobacco with a Trizol
165 reagent kit (TakaRa, Dalian, China) and was reverse-transcribed using a cDNA kit
166 (TakaRa). The experiment was executed with reaction volume of 10 μL and SYBR
167 Premix Ex TaqII (TakaRa) by using an iCycleriQ multi-color real-time PCR detection

168 system (Bio-Rad, California, CA, USA). Calculating the relative copy numbers of the
169 genes by the $2^{-\Delta\Delta Ct}$ method.[25]

170 **Differentially Expressed Proteins Analysis.** *Total Protein Extraction.* According to
171 slightly modified reported methods, the total proteins of tobacco were extracted.[26, 27] The
172 leaf sample (1.0 g) from different treatment groups were milled to homogenization in
173 liquid nitrogen, and ice-cold extraction buffer (5 mL) was added at room temperature, it
174 includes KCl of 0.1 M, Tris-HCl of 0.5 M, crose of 0.7 M, ethylene diamine tetraacetic
175 acid of 50 mM, dithiothreitol [DTT] of 40 mM, and pH was 7.5. Then the Tris-HCl (pH
176 7.5) saturated Phenol was added after 20 min of oscillation, continue to shake for 30 min
177 at 4 °C. The upper phenol layer was centrifuged for 20 min at 4500 rpm and collected
178 with a new tube, then maintain the temperature at −20 °C overnight after added the
179 methanol containing 100 mM ammonium acetate. The precipitate was collected after
180 centrifuged at 4500 rpm for 20 min at 4 °C and washed thrice under the same conditions
181 with 80% ice-cold acetone. Afterward, drying the precipitate in a vacuum drier,
182 rehydration solution (1000 μL) were added at 37 °C, it contains urea of 8 M, Tris of 0.1
183 M, DTT of 10 mM and pH was 8.5. Thereafter, Bradford method was used to determine
184 the total protein concentration. 100 μg of protein solution was collected and
185 iodoacetamide (55 mM) was added, the mixture was incubated at room temperature for
186 1 h in the dark, and centrifuged at 12,000 rpm for 20 min at 4 °C with 3 kDa Millipore.
187 The crude protein was washed six times using diluent rehydration solution. Then the
188 trypsin digest with 12.5 μg trypsin from Sigma of USA was incubated at 37 °C for 16 h.
189 Peptide solution was collected after the mixture was centrifuged at 4 °C for 20 min at
190 12,000 rpm. And then air dried, acidified by 10 μl of formic acid for further

191 chromatography–tandem MS (LC–MS/MS) analysis.

192 *Protein Identification.* Peptide samples were analyzed using a Nano LC-1DTM plus
193 system (Eksigent, Dublin, CA, USA) combined with triple time-of-flight (TOF) 5600
194 mass (AB SCIEX, Foster City, CA, USA). Furthermore, 8 μL of peptide samples was
195 obtained using a full-loop injection and desalted on a ChromXP Trap column (Nano LC
196 TRAP Column, 3 μm C18-CL, 120 Å, 350 μm × 0.5 mm, Foster City, CA, USA). Each
197 sample was eluted into a second analytical column-NanoLC-C18 reversed-phase column
198 (3C18-CL, 75 μm × 15 cm, Foster City, CA, USA) by a linear gradient formed by
199 mobile phase A (5% ACN, 0.1% FA) and mobile phase B (95% ACN, 0.1% FA) for 120
200 min at a flow rate of 300 nL/min. TripleTOF 5600 MS was operated in a data-dependent
201 mode to automatically switch between TOF–MS and product ion acquisition by utilizing
202 Analyst (R) software (TF1.6) (AB SCIEX, Foster City, CA, USA). The use of *β*-
203 galactosidase digestion for 10 minutes elution and identification of 30 min to calibrate
204 every two samples.

205 *Proteomic Data Analysis.* Analysis of LC-MS/MS data using MaxQuant version
206 1.5.2.8 (Max Planck Institute, Munich, Germany).[28] The data were searched on the basis
207 of a database consisting of the tobacco and CMV proteomes and on the basis of the
208 tobacco proteome downloaded from UniProt. The search parameters contained an initial
209 search with initial mass tolerance of 20 ppm, it set for quality recalibration.[29] The search
210 also involved an N-terminal acetylation, mutabie modification of methionine oxidation,
211 and fixed modification of carbamidomethyl cysteine. To identify the peptides, the error
212 detection rate was set to 0.01. To determine the standardized protein intensity,
213 differences in protein expression levels between the two groups were compared with

214 label-free quantification and at least two ratio counts. iBAQ algorithm is a protein
215 quantitative method, it used to sort the absolute abundance of DEPs in a single sample.[30]
216 Filtered protein tables eliminate the identification of reverse database and common
217 pollutants. To identify the accumulation of different proteins between treatment and
218 control groups, unpaired *t* test of iBAQ data of two groups was carried out.

219 *Bioinformatics analysis.* Classification of differently expressed proteins was analyzed
220 with gene ontology (GO) annotation on Kyoto Encyclopedia of Genes and Genomes
221 (KEGG) using Uniprot software. Items in GO are related of cellular component (CC),
222 biological process (BP), and molecular function (MF).[31] Differentially expressed
223 proteins (expression level > 1.5-fold) were mapped to the GO database
224 (http://www.geneontology.org/). Calculate the amount of proteins per GO term. the
225 label-free proteomics results as a target list, and generate a background list by
226 downloading the GO database.

227 **RESULTS AND DISCUSSION**

228 **Synthetic Chemistry of the Title Compounds.** Acetonitrile and $K_2CO_3$ were used as a
229 solvent and a catalyst, respectively. The corresponding substituted 4-
230 hydroxybenzaldehyde and intermediates **A1**–**A2** were stirred for 8–12 h under reflux to
231 obtain intermediates **B1**–**B12**, and the corresponding title compounds **C1**–**C28** were
232 produced by using $ZrCl_4$ as a catalyst and by condensing **B1**–**B12** with substituted
233 mercaptane (Figure 3). Their structures were identified through $^1$H NMR, $^{13}$C NMR, and
234 HRMS (Supporting Information).

235 **Antiviral Activity.** *In Vivo Anti-PVY Activity*. The antiviral activities of title
236 compounds **C1**–**C28** against PVY are shown in Table 1. Several title compounds

237 exhibited notable activities against PVY in vivo at 500 μg/mL. The curative activities of
238 **C13–C15**, **C17–C19**, **C21**, **C23**, and **C25–C27** (66.0%, 70.4%, 67.5%, 68.9%, 60.3%,
239 61.8%, 59.4%, 60.9%, 66.9%, 69.6%, and 68.6%, respectively) against PVY were
240 significantly higher than those of **6f** (58.9%), Ningnanmycin (50.6%), COS (36.3%), and
241 ribavirin (40.0%). The protective activities of **C13–C15**, **C17–C19**, and **C25–C27**
242 (60.4%, 67.6%, 62.9%, 63.6%, 58.9%, 59.8%, 62.6%, 69.4%, and 62.9%, respectively)
243 against PVY were more potent than those of **6f** (57.2%), Ningnanmycin (51.3%), COS
244 (37.2%), and ribavirin (41.2%).

245 To confirm the potential inhibitory capacity of these compounds against PVY, we
246 further evaluated $EC_{50}$ of several title compounds against PVY on the basis of previous
247 bioassays. In Table 2, the curative and protective activities of **C13–C15**, **C17**, and **C25–**
248 **C27** ($EC_{50}$ of 209.2, 125.3, 173.8, 156.7, 189.1, 130.4, and 179.6 μg/mL and 214.2, 148.4,
249 189.7, 170.1, 221.3, 152.9, and 198.7 μg/mL, respectively) against PVY were higher than
250 those of **6f** (297.6 and 281.5 μg/mL), Ningnanmycin (440.5 and 425.3 μg/mL), COS
251 (553.4 and 547.3 μg/mL), and ribavirin (677.4 and 652.7μg/mL).

252 *In Vivo Anti-CMV Activity*. The evaluation of anti-CMV activity proved that most of
253 the title compounds exerted potent inhibitory effects. In Table 2, the curative and
254 protective activities of **C13–C15**, **C17**, and **C25–C27** ($EC_{50}$ of 204.0, 108.9, 181.4, 139.2,
255 211.5, 124.7, and 209.3; and 220.1, 113.2, 190.7, 142.4, 228.1, 140.8, and 213.4 μg/mL,
256 respectively) against CMV were significantly superior to those of **6f** (259.6 and 244.3
257 μg/mL), Ningnanmycin (549.1 and 513.3 μg/mL), COS (582.8 and 570.6 μg/mL), and
258 ribavirin (690.3 and 665.4 μg/mL).

259 *In Vivo Anti-TMV Activity*. The anti-TMV activities of **C1–C28** are shown in Table 2.

260 The curative activities of **C13–C15**, **C17**, and **C25–C27** ($EC_{50}$ of 257.6, 181.7, 217.6,
261 207.8, 282.5, 229.4, and 241.4 μg/mL, respectively) against TMV were significantly
262 superior to those of **6f** (582.4 μg/mL), Ningnanmycin (373.8 μg/mL), COS (513.8 μg/mL),
263 and ribavirin (686.5 μg/mL). The protective effects of **C14** and **C17** ($EC_{50}$ of 214.6 and
264 224.7 μg/mL, respectively) against TMV were higher than those of **6f** (546.3 μg/mL),
265 Ningnanmycin (242.7 μg/mL), COS (507.9 μg/mL), and ribavirin (553.4 μg/mL).

266 **SARs.** In the dithioacetal derivatives containing a strobilurin moiety, compounds with
267 $R^2$-bearing ethyl were more favorable to antiviral activity than $R^2$-bearing aromatics
268 (**C2** > **C3**, **C4**), 2-hydroxyethyl (**C2** > **C1** and **C9** > **C8** and **C14** > **C12**, and **C17** > **C16**),
269 and other alkyls (**C14** > **C13**, **C15,** and **C17** > **C18**, **C19**). Halogen atoms substituted at
270 the 2-position of aromatic ring were more favorable to antiviral activity than electron-rich
271 groups, especially the chlorine atom **C14** > **C17** > **C2**, **C6**, **C8**, **C9**, and **C11**. This finding
272 was contradictory to those with substituent groups at the 3-position of the aromatic ring:
273 **C25** > **C23** > **C21**. Moreover, the introduction of carbon atoms instead of nitrogen atoms
274 caused the relatively decreased inhibitory activities against plant viruses as confirmed by
275 the following pattern: **C26** < **C14** and **C27** < **C15** and **C28** < **C17**.

276 **Physiological and Biochemical Analysis of Tobacco.** *Effect on Chlorophyll Contents.*
277 Chlorophyll is a core chloroplast component that plays a key role in photosynthesis. The
278 chlorophylls comprised $C_a$, $C_b$, $C_t$, and $C_{a/b}$ was tested in this study. The chlorophyll
279 content decreased gradually after tobacco plants were inoculated with CMV (Figure 3).
280 However, from day 1 to day 7, the chlorophyll content had increased, and reached the
281 maximum on day 5 after the CMV-inoculated tobacco leaves were treated with **C14**. The
282 trend of **C14** therapy was better than that of COS treatment. Hence, **C14** might enhance

283 the resistance of the plant host to diseases by increasing the chlorophyll content.

284 *Effect on Defensive Enzyme Activities.* CAT, POD, SOD, and PAL are several important
285 defense enzymes, whose enhanced activities are significantly related to inducible
286 resistance. Antioxidant defense machinery can protect plant from oxidative damage
287 caused by reactive oxygen species (ROS).[32] In this study, the defensive enzyme activities
288 of tobacco after **C14** treatment were analyzed. CAT can decomposed into water and
289 oxygen by catalyzing hydrogen peroxide to protect host from oxidative damage to ROS.[33]
290 The CAT activities of **C14** treatment groups were 1.90, 1.31, 1.27, and 1.99 times as
291 much as that of the control groups after 1, 3, 5, and 7 days, respectively. From 1day to 5
292 day, the values were increased and reached the maximum on 5 day (Figure 5A). POD can
293 reduce the hydrogen peroxide content in the plant body.[34] The POD activities of **C14**
294 treatment groups were 1.05, 2.01, 2.38, and 1.38 times as much as that of the control
295 group on day 1, 3, 5, and 7, respectively, and the maximum were obtained on day 5
296 (Figure 5B). The SOD activities of **C14** treatment groups were 1.78, 1.95, and 1.05 times
297 that of the control groups after 3, 5, and 7 days, respectively (Figure 5C). The PAL
298 activities after **C14** treatment was administered did not significantly change (Figure 5D).
299 The results demonstrated that **C14** could improve the resistance of tobacco to the virus
300 through defense response induced by the enhanced activities of enzymes, especially POD
301 and SOD.

302 **RT-qPCR analysis.** As representatives of the sample on day 5, to study the mechanism
303 of **C14** response in CMV-infected tobacco, the relative expression levels of the defense
304 genes of NPR-1, CAT-1, PAL-1, isochorismate synthase 1 (ICS-1), enhanced disease
305 susceptibility 1 (EDS-1), and SOD were investigated through reverse transcription (RT-

306 qPCR). In Figure 6, the relative expression levels of CAT-1, ICS-1, and SOD of **C14**
307 treatment groups were higher than the CK and COS control groups. The relative
308 expression of SOD in the treatment group was about 4.00 and 3.36 times more that of CK
309 and COS. The relative expression of CAT-1 and ICS-1 increased by approximately 1.32
310 and 1.57 times and by 2.00 and 2.07 times, respectively. These results demonstrated that
311 **C14** could improve the disease resistance of tobacco by inducing defense-related proteins,
312 namely, CAT-1, ICS-1, and SOD.

313 **Analysis of Proteomics** MaxQuant version 1.5.2.8 (Max Planck Institute, Munich,
314 Germany) was used to search for peptide results, and 2088 proteins were found and
315 quantified. As showed of Figure 7, a total of 1706 and 1676 proteins were identified in
316 the control and treatment groups, respectively. In the total proteins, 412 (19.7%) and 382
317 (18.3%) were specifically expressed in CK and **C14** groups, respectively. A volcanic map
318 was plotted to understand the differential protein expression levels (Figure 8). Of the total
319 number of identified differentially expressed proteins, 412 were downregulated (blue dots)
320 and 382 were upregulated (red dots) (fold change > 1.5, $p < 0.05$) in the treatment and
321 control groups (Supporting Information-II).

322 **Bioinformatics Analysis of the Control and Treatment Groups**. The expressed
323 proteins were annotated using the Database for Annotation Differentially, Visualization,
324 and Integrated Discovery 6.8 (DAVID 6.8). On the basis of the GO categories, we
325 analyzed the differentially expressed proteins identified in CC, BP, and MF in the
326 treatment and control groups.[35] Figure 9 shows the GO term enrichment analysis of
327 differentially expressed proteins (DEPs, $P < 0.05$). The DEPs in the cytoplasm,
328 membrane, nucleus, photosystem, chloroplast, mitochondrion, cytosol, extracellular

329 region, and plasma membrane were grouped according to their CC (Figure 9A). The
330 DEPs involved in the generation of precursor metabolites and energy, photosynthesis,
331 transport, signal transduction, response to oxidative stress, defense response, lipid
332 metabolism, and response to stress were categorized on the basis of their BP (Figure 9B).
333 The differently expressed proteins involved in RNA binding, DNA binding, enzyme
334 regulator activity, kinase activity, protein binding, nuclease activity, transporter activity,
335 ATPase activity, and signal transducer activity were classified on the basis of their MF
336 (Figure 9C).

337 **Functional Classification by KEGG.** KEGG was used to research the response to the
338 action of **C14** and determine the way of action triggered by **C14**. In Figure 10 and Table 3,
339 several specific proteins, including ABC transporter F family member 1 (ABC proteins),
340 calcium-dependent protein kinase 2-like (CDPKs), and superoxide dismutase (SOD, EC
341 1.15.1.1) were upregulated. These proteins play key roles in the abscisic acid (ABA)
342 signaling pathway. Few studies have shown that ABA levels in a virally infected host
343 plant can increase, thereby demonstrating the involvement of ABA in antivirus defense of
344 plants.[36, 37] A previous study revealed that ABC proteins are key transmembrane
345 transporters, which can transport ABA from the outer compartment to the inner
346 compartment to participate in ABA signaling.[38] Afterward, PP2Cs function as negative
347 regulators to repress ABA signaling and bind to PYR/PYL/RCAR receptors. The function
348 of SnRK2s is dependent on PYR/PYL/RCAR receptors in ABA signaling pathway.[39, 40]
349 CDPKs are $Ca^{2+}$ sensors that are universal and evolutionarily conserved and implicated as
350 main regulators of $Ca^{2+}$-mediated ABA and stress responses essential for plant survival.[41]
351 CDPKs can regulate ABA-mediated gene expression though ABFs, which are ABA-

352 responsive transcription factors that serve as substrates of several CDPKs.[42] The present
353 study demonstrated that SOD was upregulated in the treatment groups. A previous study
354 indicated that ABA causes an increase in the sustained SOD.[43] CDPKs are involved in
355 ABA-induced upregulation of SOD activity and expression.[44] The disproportionation of
356 superoxide to molecular oxygen and hydrogen peroxide can be catalyed by SOD, which
357 constitute an antioxidant defense system with defense enzymes, such as CAT and POD.
358 The antioxidant defense system protects plants against oxidative damage by scavenging
359 ROS.[45, 46] ABA accumulation can increase the generation of ROS and the induction of
360 several antioxidant enzymes.[47] In the present study, heat shock proteins (HSPs) were
361 downregulated in the treatment groups. The expression of HSPs is ABA dependent, and
362 they negatively regulate ABA response.[48]

363 On the basis of the broad bioactivity of strobilurins and the lead compound **6f**, we
364 designed and synthesized 28 novel dithioacetal derivatives bearing a strobilurin moiety.
365 Bioassay results indicated that the antiviral potency of **C14** against CMV and PVY were
366 superior to those of **6f**, Ningnanmycin, COS, and ribavirin. Meanwhile, compound **C14**
367 can be used to control TMV. This antiviral activity was associated with an increase in the
368 content of the chlorophyll and the enhanced activity of defensive enzyme in tobacco
369 treated with **C14**. RT-qPCR analysis revealed the relative expression levels of SOD in the
370 **C14** treatment groups were higher than those of the CK and COS control groups. This
371 discovery has been confirmed by the specific expression of the stress responses and
372 related proteins of abscisic acid signaling pathway. In this paper, we demonstrated that
373 **C14** can enhance the tolerance of plants to CMV infection by inducing the accumulation
374 of ABA. Therefore, **C14** can be considered as a new type of antiviral agent.

375 **ASSOCIATED CONTENT**

376 **Supporting Information**

377 Characterization data, $^{1}H$ and $^{13}C$ NMR spectra, and HRMS for intermediates **B1–B12**
378 and title compounds **C1–C28** are provided. Supplementary data associated with this
379 article can be found in the online version at http://pubs.acs.org.

380 All of the identified proteins, GO term enrichment analysis, and differential protein
381 expression in the treatment group compared with that in the control group are listed in
382 Supporting Information-II.

383

384 **ACKNOWLEDGMENTS**

385 The authors gratefully acknowledge the National Natural Science Foundation of China
386 (No, 21562013)

387 **Notes**

388 The authors declare no competing financial interest.

389

390 **REFERENCES**

391 (1) Tomlinson, J. A. Epidemiology and control of virus diseases of vegetables. *Ann. Appl.*
392 *Biol.* **1987**, *110*, 661−681.

393 (2) Kennedy, J. S. A biological approach to plant viruses. *Nature* **1951**, *168*, 890−894.

394 (3) Harrison, B. D.; Mayo, M. A.; Baulcombe, D. C. Virus resistance in transgenic plants
395 that express cucumber mosaic virus satellite RNA. *Nature* **1987**, *328*, 799−802.

396 (4) Scholthof, K. B. G.; Adkins, S.; Czosnek, H.; Palukaitis, P.; Jacquot, E.; Hohn, T.;
397 Hohn, B.; Saunders, K.; Candresse, T.; Ahlquist, P.; Hemenway, C.; Foster, G. D. Top

398 10 plant viruses in molecular plant pathology. *Mol. Plant Pathol.* **2011**, *12*, 938–954.
399 (5) Su, B.; Cai, C. L.; Deng, M.; Wang, Q. M. Spatial configuration and three-
400 dimensional conformation directed design, synthesis, antiviral activity, and structure-
401 activity relationships of phenanthroindolizidine analogues. *J. Agric. Food Chem.*
402 **2016**, *64*, 2039−2045.
403 (6) Yang, A. M.; Yu, L.; Chen, Z.; Zhang, S. X.; Shi, J.; Zhao, X. Z.; Yang, Y. Y.; Hu, D.
404 Y.; Song, B. A.; Label-free quantitative proteomic analysis of chitosan
405 oligosaccharide-treated rice infected with southern rice black-streaked dwarf virus.
406 *Viruses* **2017**, *9*, 115.
407 (7) Wu, M.; Han, G. F.; Wang, Z. W.; Liu, Y. X.; Wang, Q. M. Synthesis and antiviral
408 activities of antofine analogues with different C-6 substituent groups. *J. Agric. Food*
409 *Chem*. **2013**, *61*, 1030−1035.
410 (8) Yan, X. H.; Chen, J.; Di, Y. T.; Fang, X.; Dong, J. H.; Sang, P.; Wang Y. H.; He, H. P.;
411 Zhang, Z. K.; Hao, X. J. Anti-tobacco mosaic virus (TMV) quassinoids from *Brucea*
412 *javanica* (L.) Merr. *J. Agric. Food Chem.* **2010**, *58*, 1572−1577.
413 (9) Li, Y. M.; Zhang, Z. K.; Jia, Y. T.; Shen, Y. M.; He, H. P.; Fang, R. X.; Chen, X. Y.;
414 Hao, X. J. 3-Acetonyl-3-hydroxyoxindole: a new inducer of systemic acquired
415 resistance in plants. *Plant Biotechnol. J.* **2008**, *6*, 301−308.
416 (10) Zhang, J.; Zhao, L.; Zhu, C.; Wu, Z. X.; Zhang, G. P.; Gan, X. H.; Liu, D. Y.; Pan, J.
417 K.; Hu, D. Y.; Song, B. A. Facile Synthesis of novel vanillin derivatives
418 incorporating a bis(2-hydroxyethyl)dithioacetal moiety as antiviral agents. *J. Agric.*
419 *Food Chem.* **2017**, *65*, 4582−4588.
420 (11) Li, M.; Liu, C. L.; Yang, J. C.; Zhang, J. B.; Li, Z. N.; Zhang, H.; Li, Z. M. Synthesis

421 and biological activity of new (*E*)-*α*-(methoxyimino) benzeneacetate derivatives
422 containing a substituted pyrazole ring. *J. Agric. Food Chem.* **2010**, *58*, 2664−2667.
423 (12) Liu, A. P.; Wang, X. G.; Ou, X. M.; Huang, M. Z.; Chen, C.; Liu, S. D.; Huang, L.;
424 Liu, X. P.; Zhang, C. L.; Zheng, Y. Q.; Ren, Y. G.; He, L.; Yao, J. R. Synthesis and
425 fungicidal activities of novel bis(trifluoromethyl) phenyl-based strobilurins. *J.*
426 *Agric. Food Chem.* **2008**, *56*, 6562−6566.
427 (13) Debona, D.; Nascimento, K. J. T.; Gomes, J. G. O.; Aucique-Perez, C. E.; Rodrigues,
428 F. A. Physiological changes promoted by a strobilurin fungicide in the rice-*Bipolaris*
429 *oryzae* interaction. *Pestic. Biochem. Phys.* **2016**, *130*, 8−16.
430 (14) Zhao, P. L.; Wang, F.; Zhang, M. Z.; Liu, Z. M.; Huang, W.; Yang, G. F. Synthesis,
431 fungicidal, and insecticidal activities of *β*-methoxyacrylate-containing *N*-acetyl
432 pyrazoline derivatives. *J. Agric. Food Chem.* **2008**, *56*, 10767−10773.
433 (15) Chai, B. S.; Liu, C. L.; Li, H. C.; Liu, S. W.; Xu, Y.; Song, Y. Q.; Chang, J. B.
434 Synthesis and acaricidal activity of strobilurin-pyrimidine derivatives. *Chinese Chem.*
435 *Lett.* **2014**, *25*, 137−140.
436 (16) Wu, Q. Y.; Wang, G. D.; Huang, S. W.; Lin, L.; Yang, G. F. Synthesis and biological
437 activity of novel phenyltriazolinone derivatives. *Molecules* **2010**, *15*, 9024−9034.
438 (17) Herms, S.; Seehaus, K.; Koehle, H.; Conrath, U. A strobilurin fungicide enhances the
439 resistance of tobacco against tobacco mosaic virus and *Pseudomonas syringae* pv
440 tabaci. *Plant Physiol.* **2002**, *130*, 120−127.
441 (18) Zhao, P. L.; Liu, C. L.; Huang, W.; Wang, Y. Z.; Yang, G. F. Synthesis and fungicidal
442 evaluation of novel chalcone-based strobilurin analogues. *J. Agric. Food Chem.*
443 **2007**, *55*, 5697−5700.

(19) Huang, W.; Zhao, P. L.; Liu, C. L.; Chen, Q.; Liu, Z. M.; Yang, G. F. Design, synthesis, and fungicidal activities of new strobilurin derivatives. *J. Agric. Food Chem.* **2007**, *55*, 3004−3010.

(20) Lu, G. H.; Chu, H. B.; Chen, M.; Yang, C. L. Synthesis and bioactivity of novel strobilurin derivatives containing the pyrrolidine-2, 4-dione moiety. *Chinese Chem. Lett.* **2014**, *25*, 61−64.

(21) Iannelli, D.; D'Apice, L.; Cottone, C.; Viscardi, M.; Scala, F.; Zoina, A.; Del Sorbo, G.; Spigno, P.; Capparelli, R. Simultaneous detection of cucumber mosaic virus, tomato mosaic virus and potato virus Y by flow cytometry. *J. Virol. Methods* **1997**, *69*, 137−145.

(22) Scott, H. Purification of cucumber mosaic virus. *Virology* **1963**, *20*, 103−106.

(23) Gooding, G. V., Jr.; Hebert, T. T. A simple technique for purification of tobacco mosaic virus in large quantities. *Phytopathology* **1967**. *57*. 1285–1287.

(24) Wu, Z. X.; Zhang, J.; Chen, J. X.; Pan, J. K.; Zhao, L.; Liu, D. Y.; Zhang, A. W.; Chen, J.; Hu, D. Y.; Song, B. A. Design, synthesis, antiviral bioactivity and three-dimensional quantitative structure-activity relationship study of novel ferulic acid ester derivatives containing quinazoline moiety. *Pest Manag. Sci.* **2017**, *73*, 2079−2089.

(25) Livak, K. J.; Schmittgen, T. D. Analysis of relative gene expression data using real-time quantitative PCR and the $2^{-\Delta\Delta CT}$ method. *Methods* **2001**, *25*, 402−408.

(26) Tahara, S. T.; Mehta, A.; Rosato, Y. B. Proteins induced by *Xanthomonas axonopodis* pv. *passiflorae* with leaf extract of the host plant (*Passiflorae edulis*). *Proteomics* **2003**, *3*, 95−102.

467 (27) Qian, G. L.; Zhou, Y. J.; Zhao, Y. C.; Song, Z. W.; Wang, S. Y.; Fan, J. Q.; Hu, B.
468 S.; Venturi, V.; Liu, F. Q. Proteomic analysis reveals novel extracellular virulence-
469 associated proteins and functions regulated by the diffusible signal factor (DSF) in
470 *Xanthomonas oryzae* pv. *oryzicola*. *J. Proteome Res.* **2013**, *12*, 3327−3341.
471 (28) Cox, J.; Neuhauser, N.; Michalski, A.; Scheltema, R. A.; Olsen, J. V.; Mann, M.
472 Andromeda: a peptide search engine integrated into the MaxQuant environment. *J.*
473 *Proteome Res.* **2011**, *10*, 1794−1805.
474 (29) Cox, J.; Michalski, A.; Mann, M. Software lock mass by two-dimensional
475 minimization of peptide mass errors. *J. Am. Soc. Mass Spectrom.* **2011**, *22*,
476 1373−1380.
477 (30) Luber, C. A.; Cox, J.; Lauterbach, H.; Fancke, B.; Selbach, M.; Tschopp, J.; Akira,
478 S.; Wiegand, M.; Hochrein, H.; O'Keeffe, M.; Mann, M. Quantitative proteomics
479 reveals subset-specific viral recognition in dendritic cells. *Immunity* **2010**, *32*,
480 279−289.
481 (31) Consortium, G. O. The gene ontology (GO) database and informatics resource.
482 *Nucleic Acids Res*. **2004**, *32*, 258−261.
483 (32) Apel, K.; Hirt, H. Reactive oxygen species: metabolism, oxidative stress, and signal
484 transduction. *Annu. Rev. Plant Biol.* **2004**, *55*, 373−399.
485 (33) Wheeler, C. R.; Salzman, J. A.; Elsayed N M, Omaye, S. T.; Korte, D. W. Jr.
486 Automated assays for superoxide dismutase, catalase, glutathione peroxidase, and
487 glutathione reductase activity. *Anal. Biochem.* **1990**, *184*, 193−199.
488 (34) Kawano, T. Roles of the reactive oxygen species-generating peroxidase reactions in
489 plant defense and growth induction. *Plant Cell Rep.* **2003**, *21*, 829−837.

490 (35) Thissen, D.; Steinberg, L.; Kuang, D. Quick and easy implementation of the
491 Benjamini-Hochberg procedure for controlling the false positive rate in multiple
492 comparisons. *J. Educ. Behav. Stat.* **2002**, *27*, 77−83.
493 (36) Zhang, H. B.; Zhu, X. R.; Liu, H. X. Effect of banana bunchy top virus (BBTV) on
494 endogenous hormone of banana plant. *Acta Phytopathol Sin.* **1997**, *27*, 79–83.
495 (37) Whenham, R. J.; Fraser, R. S. S.; Brown, L. P.; Payne, J. A. Tobacco-mosaic-virus-
496 induced increase in abscisic-acid concentration in tobacco leaves: Intracellular
497 location in light and dark-green areas, and relationship to symptom development.
498 *Planta* **1986**, *168*, 592–598.
499 (38) Tardieu, F. Parent, B. Simonneau, T. Control of leaf growth by abscisic acid:
500 hydraulic or non−hydraulic processes? *Plant Cell Environ.* **2010**, *33*, 636–647.
501 (39) Park, S. Y.; Fung, P.; Nishimura, N.; Jensen, D. R.; Fujii, H.; Zhao, Y.; Lumba, S.;
502 Santiago, J.; Rodrigues, A.; Chow, T. F.; Alfred, S. E.; Bonnetta, D.; Finkelstein, R.;
503 Provart, N. J.; Desveaux, D.; Rodriguez, P. L.; McCourt, P.; Zhu, J. K.; Schroeder, J.
504 I.; Volkman, B. F.; Cutler, S. R. Abscisic acid inhibits PP2Cs via the PYR/PYL
505 family of ABA-binding START proteins. *Science* **2009**, *324*, 1068–1071.
506 (40) Gonzalez-Guzman, M.; Pizzio, G. A.; Antoni, R.; Vera-Sirera, F.; Merilo, E.; Bassel,
507 G. W.; Fernández, M. A.; Holdsworth, M. J.; Perez-Amador, M. A.; Kollist, H.;
508 Rodriguez, P. L. *Arabidopsis* PYR/PYL/RCAR receptors play a major role in
509 quantitative regulation of stomatal aperture and transcriptional response to abscisic
510 acid. *Plant Cell* **2012**, *24*, 2483–2496.
511 (41) Zou, J. J.; Wei, F. J.; Wang, C.; Wu, J. J.; Ratnasekera, D.; Liu, W. X.; Wu, W. H.

512 Arabidopsis calcium-dependent protein kinase CPK10 functions in abscisic acid-
513 and $Ca^{2+}$-mediated stomatal regulation in response to drought stress. *Plant Physiol.*
514 **2010**, *154*, 1232–1243.
515 (42) Zhu, S. Y.; Yu, X. C.; Wang, X. J.; Zhao, R.; Li, Y.; Fan, R. C.; Shang, Y.; Du, S. Y.;
516 Wang, X. F.; Wu, F. Q.; Xu, Y. H.; Zhang, X. Y.; Zhang, D. P. Two calcium-
517 dependent protein kinases, CPK4 and CPK11, regulate abscisic acid signal
518 transduction in *Arabidopsis*. *Plant Cell* **2007**, *19*, 3019–3036.
519 (43) Choudhary, R.; Saroha, A. E.; Swarnkar, P. L. Effect of abscisic acid and hydrogen
520 peroxide on antioxidant enzymes in *Syzygium cumini* plant. *J. Food Sci. Technol.*
521 **2012**, *49*, 649–652.
522 (44) Ding, Y. F; Cao, J. M; Ni, L.; Zhu, Y.; Zhang, A. Y; Tan, M. P; Jiang, M. Y.
523 ZmCPK11 is involved in abscisic acid-induced antioxidant defence and functions
524 upstream of ZmMPK5 in abscisic acid signalling in maize. *J. Exp. Bot.* **2013**, *64*,
525 871–884.
526 (45) Foyer, C. H.; Noctor, G. Redox homeostasis and antioxidant signaling: a metabolic
527 interface between stress perception and physiological responses. *Plant Cell* **2005**, *17*,
528 1866–1875.
529 (46) Foyer, C. H.; Descourvières, P.; Kunert, K. J. Protection against oxygen radicals: an
530 important defence mechanism studied in transgenic plants. *Plant Cell Environ.* **1994**,
531 *17*, 507–523.
532 (47) Jiang, M. Y.; Zhang, J. H. Role of abscissic acid in water stress-induced antioxidant
533 defense in leaves of maize seedlings. *Free Radical. Res.* **2002**, *36*, 1001–1015.
534 (48) Li, Y. L; Li, Y. Q.; Liu, Y. C.; Wu, Y. R.; Xie, Q. The sHSP22 heat-shock protein

requires the ABI1 protein phosphatase to modulate polar auxin transport and downstream responses. *Plant Physiol.* **2018**, *176*, 2406–2425.

538 **FIGURE CAPTIONS**

539 **Figure 1.** Chemical structures of Chitosan oligosaccharide, Ribavirin, and Ningnanmycin.

540 **Figure 2.** Design of the title compounds.

541 **Figure 3.** Synthetic route of dithioacetal derivatives bearing strobilurin moiety.

542 **Figure 4.** Effects of compound **C14** on $C_a$ (A), $C_b$ (B), $C_t$ (C), and Chlorophyll $_{a/b}$ (D) in
543 tobacco leaves. Vertical bars refer to mean ± SD ($n$ = 3).

544 **Figure 5.** Effects of compound **C14** on CAT (A), POD (B), SOD (C), and PAL (D)
545 activity in tobacco leaves. Vertical bars refer to mean ± SD ($n$ = 3).

546 **Figure 6.** Gene expression analysis of the related genes by RT-qPCR. The genes
547 expression levels of CAT-1, ICS-1, and SOD were up-regulated by **C14** treatment.

548 **Figure 7.** Changed proteome distribution between **C14** and CK, Venn diagram showing
549 unique and shared proteins.

550 **Figure 8.** Volcano plot of the relative protein abundance changes between control group
551 and treatment group. The red points are significant up-regulated proteins, while the green
552 points are significant down-regulated proteins

553 **Figure 9.** The differential expression proteins between control and treatment group were
554 classified based on known cellular components (A), biological process (B) and molecular
555 functions (C).

556 **Figure 10.** The ABA signaling pathway in tobacco response to **C14**. Red color represent
557 up-accumulated proteins in this pathway, while the green color represent down-
558 accumulated.

559

560

**Table 1 Antiviral activity of the title compounds against PVY, CMV, and TMV at 500 $\mu$g/mL[a]**

| Compd. | 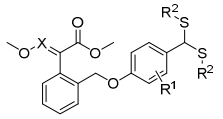 | | | Anti-PVY | | Anti-CMV | | Anti-TMV | |
|---|---|---|---|---|---|---|---|---|---|
| | $R^1$ | $R^2$ | X | curative activity (%) | protective activity (%) | curative activity (%) | protective activity (%) | curative activity (%) | protective activity (%) |
| **C1** | 2-$OCH_3$ | 2-hydroxyethyl | N | 38.5±2.3 | 37.2±3.0 | 38.0±2.6 | 33.5±3.9 | 36.9±5.4 | 37.3±4.9 |
| **C2** | 2-$OCH_3$ | Et | N | 46.7±1.7 | 44.2±3.2 | 49.3±2.5 | 45.5±3.3 | 46.7±2.5 | 47.0±5.9 |
| **C3** | 2-$OCH_3$ | 4-F-Ph | N | 41.2±3.2 | 39.5±2.6 | 40.0±1.8 | 39.6±2.6 | 41.6±2.6 | 42.2±4.0 |
| **C4** | 2-$OCH_3$ | Bn | N | 42.2±1.4 | 40.9±3.7 | 41.1±2.6 | 40.8±2.8 | 42.6±4.9 | 43.3±2.2 |
| **C5** | - | 2-hydroxyethyl | N | 35.6±1.1 | 32.0±3.2 | 30.5±3.6 | 29.6±2.2 | 32.7±3.1 | 34.2±5.3 |
| **C6** | - | Et | N | 44.3±2.8 | 40.2±4.9 | 42.5±1.3 | 43.6±4.1 | 42.5±2.5 | 40.6±3.7 |
| **C7** | 2-$CH_3$ | 2-hydroxyethyl | N | 39.2±2.1 | 40.1±1.3 | 38.6±2.7 | 37.5±1.9 | 39.6±2.6 | 38.3±2.1 |
| **C8** | 2-$CH_3$ | Et | N | 52.1±1.9 | 50.9±2.6 | 52.5±2.5 | 50.2±1.3 | 52.8±3.1 | 54.3±2.4 |
| **C9** | 2-OEt | Et | N | 44.6±2.8 | 43.9±4.3 | 40.3±2.0 | 42.2±1.3 | 41.2±2.7 | 52.8±2.3 |
| **C10** | 2,6-di$OCH_3$ | 2-hydroxyethyl | N | 25.4±3.7 | 24.9±3.1 | 30.8±3.3 | 29.2±3.1 | 26.3±2.9 | 27.5±4.0 |
| **C11** | 2,6-di$OCH_3$ | Et | N | 40.2±4.1 | 41.6±3.4 | 38.0±1.0 | 38.4±2.5 | 33.9±4.2 | 32.1±2.9 |
| **C12** | 2-Cl | 2-hydroxyethyl | N | 47.6±3.2 | 49.8±1.5 | 43.8±3.4 | 44.5±2.9 | 44.6±3.5 | 40.0±2.2 |
| **C13** | 2-Cl | Pr | N | 66.0±2.3 | 60.4±1.9 | 64.9±1.2 | 63.5±2.5 | 59.2±4.0 | 56.7±2.1 |
| **C14** | 2-Cl | Et | N | 70.4±1.3 | 67.6±2.5 | 71.5±2.3 | 70.9±3.9 | 67.3±3.3 | 63.9±2.4 |
| **C15** | 2-Cl | *i*-Pr | N | 67.5±4.6 | 62.9±2.3 | 68.2±2.3 | 66.3±3.5 | 59.3±4.2 | 57.2±2.5 |
| **C16** | 2-Br | 2-hydroxyethyl | N | 43.7±3.7 | 40.4±3.1 | 41.8±3.9 | 40.2±2.1 | 43.2±2.4 | 44.6±1.8 |
| **C17** | 2-Br | Et | N | 68.9±2.5 | 63.6±1.4 | 60.4±5.6 | 58.8±6.0 | 60.3±4.0 | 59.7±2.4 |
| **C18** | 2-Br | Pr | N | 60.3±3.1 | 58.9±2.4 | 55.4±2.3 | 53.7±1.6 | 55.2±4.1 | 51.4±2.9 |
| **C19** | 2-Br | *i*-Pr | N | 61.8±2.8 | 59.8±1.6 | 56.3±4.1 | 54.3±2.3 | 56.7±2.8 | 53.3±3.9 |
| **C20** | 3-Cl | 2-hydroxyethyl | N | 43.0±1.1 | 39.5±2.8 | 39.5±4.1 | 37.2±4.2 | 38.5±2.5 | 39.3±4.5 |
| **C21** | 3-Cl | Et | N | 59.4±3.2 | 56.2±2.7 | 56.4±3.2 | 55.2±2.0 | 44.1±2.6 | 45.0±3.0 |
| **C22** | 3-$CH_3$ | 2-hydroxyethyl | N | 43.3±3.0 | 42.1±4.1 | 40.1±3.8 | 39.2±2.6 | 38.4±2.6 | 40.1±2.1 |
| **C23** | 3-$CH_3$ | Et | N | 60.9±4.3 | 57.3±3.1 | 57.2±3.2 | 56.5±3.1 | 53.2±4.1 | 52.1±2.3 |
| **C24** | 3-$OCH_3$ | 2-hydroxyethyl | N | 45.9±3.1 | 42.5±3.4 | 48.7±3.7 | 45.7±2.0 | 44.0±3.9 | 43.6±3.1 |
| **C25** | 3-$OCH_3$ | Et | N | 66.9±2.1 | 62.6±2.8 | 64.3±3.5 | 62.2±2.8 | 59.4±3.2 | 60.2±2.1 |
| **C26** | 2-Cl | Et | CH | 69.6±3.3 | 69.4±2.4 | 69.1±3.5 | 66.5±3.8 | 59.2±3.5 | 59.0±2.4 |
| **C27** | 2-Cl | *i*-Pr | CH | 68.6±3.6 | 62.9±4.2 | 68.2±4.3 | 67.0±3.6 | 57.5±3.3 | 56.1±2.1 |
| **C28** | 2-Br | Et | CH | 56.3±3.6 | 54.3±4.2 | 55.1±4.3 | 56.9±3.6 | 54.9±3.0 | 53.1±2.4 |
| **6f**[b] | - | - | - | 58.9±3.2 | 57.2±1.5 | 58.3±3.4 | 56.5±2.8 | 45.8±2.3 | 46.1±1.4 |
| **Ningnanmycin**[c] | - | - | - | 50.6±3.4 | 51.3±3.1 | 48.9±5.4 | 49.3±2.7 | 56.6±2.3 | 65.8±3.4 |
| COS[d] | - | - | - | 36.3±1.6 | 37.2±2.0 | 34.5±1.4 | 35.3±2.1 | 33.5±2.2 | 34.4±1.9 |
| **Ribavirin**[e] | - | - | - | 40.0±2.1 | 41.2±2.3 | 38.5±1.6 | 39.7±1.8 | 40.2±2.3 | 42.6±1.5 |

[a]Average of three replicates; [b]**6f**, [c]Ningnanmycin, [d]COS, and [e]Ribavirin were used as control.

567 **Table 2 $EC_{50}$ values of the title compounds against PVY, CMV, and TMV[a] ($\mu$g/mL)**

| Compd. | $EC_{50}$ for PVY | | $EC_{50}$ for CMV | | $EC_{50}$ for TMV | |
|---|---|---|---|---|---|---|
| | curative activity | protective activity | curative activity | protective activity | curative activity | protective activity |
| **C1** | 1426.2±7.8 | 1520.5±5.0 | 1472.3±9.7 | 1674.6±5.7 | 1356.2±9.3 | 1525.3±4.9 |
| **C2** | 617.1±10.9 | 633.8±8.4 | 651.2±9.2 | 679.8±7.7 | 628.6±5.8 | 609.8±9.4 |
| **C3** | 1024.4±5.4 | 1103.7±3.4 | 1248.4±4.9 | 1189.7±9.1 | 1109.5±8.1 | 1288.3±4.9 |
| **C4** | 1289.4±6.1 | 1455.3±3.7 | 1492.5±10.3 | 1308.1±9.4 | 1189.2±6.7 | 1267.5±8.3 |
| **C8** | 432.1±8.4 | 450.6±5.1 | 428.7±7.5 | 441.4±6.6 | 581.7±7.3 | 540.6±4.7 |
| **C9** | 670.9±7.8 | 696.3±7.7 | 682.6±6.7 | 690.6±5.4 | 684.7±4.8 | 673.8±6.6 |
| **C11** | 700.5±8.6 | 749.6±6.5 | 785.0±4.0 | 804.9±8.1 | 952.5±9.4 | 987.4±11.3 |
| **C12** | 626.4±6.6 | 638.3±3.9 | 556.2±4.9 | 628.1±9.1 | 618.4±9.4 | 639.2±8.3 |
| **C13** | 209.2±4.0 | 214.2±6.7 | 204.0±6.7 | 220.1±4.2 | 257.6±6.9 | 282.1±7.2 |
| **C14** | 125.3±4.9 | 148.4±5.5 | 108.9±6.1 | 113.2±7.9 | 181.7±5.7 | 214.6±4.9 |
| **C15** | 173.8±7.4 | 189.7±4.4 | 181.4±4.1 | 190.7±4.7 | 217.6±8.4 | 247.8±6.4 |
| **C16** | 640.2±11.3 | 657.6±5.1 | 628.6±7.9 | 648.0±10.4 | 648.2±5.4 | 652.7±6.1 |
| **C17** | 156.7±8.4 | 170.1±5.4 | 139.2±8.1 | 142.4±9.2 | 207.8±5.1 | 224.7±8.5 |
| **C18** | 325.6±9.7 | 349.6±6.7 | 319.6±7.2 | 328.3±7.6 | 386.7±9.0 | 382.1±9.7 |
| **C19** | 302.4±8.0 | 322.0±4.9 | 256.7±5.7 | 274.8±7.0 | 377.9±7.3 | 342.8±10.7 |
| **C21** | 315.1±8.8 | 341.9±6.8 | 345.6±10.7 | 367.1±7.3 | 422.4±8.2 | 448.7±7.7 |
| **C23** | 297.5±7.9 | 304.6±6.1 | 270.2±8.5 | 284.7±5.1 | 406.7±11.4 | 418.4±8.5 |
| **C25** | 189.1±7.9 | 221.3±6.3 | 211.5±9.8 | 228.1±7.0 | 282.5±5.8 | 301.4±6.7 |
| **C26** | 130.4±6.1 | 152.9±10.4 | 124.7±7.9 | 140.8±7.9 | 229.4±5.3 | 241.7±9.4 |
| **C27** | 179.6±4.0 | 198.7±9.9 | 209.3±6.4 | 213.4±8.6 | 241.4±10.7 | 257.5±8.9 |
| **C28** | 299.6±4.8 | 290.1±6.8 | 264.0±8.2 | 266.1±6.4 | 372.7±9.4 | 408.9±5.3 |
| **6f**[b] | 297.6±2.5 | 281.5±1.7 | 259.6±4.1 | 244.3±1.2 | 582.4±4.8 | 546.3±2.5 |
| **Ningnanmycin**[c] | 440.5±2.0 | 425.3±2.4 | 549.1±4.5 | 513.3±3.2 | 373.8±2.1 | 242.7±1.1 |
| COS[d] | 553.4±4.6 | 547.3±5.6 | 582.8±4.1 | 570.6±6.7 | 513.8±3.6 | 507.9±3.9 |
| **Ribavirin**[e] | 677.4±6.5 | 652.7±5.8 | 690.3±7.2 | 665.4±5.6 | 686.5±5.2 | 653.4±6.2 |

568 [a]Average of three replicates; [b]Used as control; [c]Used as control; [d]Used as control; [e]Used as control.

569

570 **Table 3 DEPs Involved in Abscisic acid signaling pathway.**

| Protein ID | Protein Names | Length | LogRatio | LogP | Sig |
|---|---|---|---|---|---|
| **A0A1S4CII8_TOBAC** | ABC transporter I family member 6, chloroplastic-like | 320 | 10 | - | up |
| **A0A1S4AD21_TOBAC** | ABC transporter F family member 1 | 602 | 10 | - | up |
| **A0A1S4BCT9_TOBAC** | calcium-dependent protein kinase2-like | 521 | 1.613536 | 3.03479 | up |
| **A0A1S4DIN0_TOBAC** | Superoxide dismutase (EC 1.15.1.1) | 228 | 10 | - | up |
| **A0A1S4DS24_TOBAC** | Superoxide dismutase (EC 1.15.1.1) | 246 | 2.305384 | 1.419729 | up |
| **A0A1S3ZDE0_TOBAC** | heat shock protein 90-5, chloroplastic-like | - | - | - | down |

571

572

## Table of Contents Graphic